Advances in Magnetic Resonance Imaging: From Low-Field to High-Field and Back to Low-Field MRI

Yasuhiko Terada
(Faculty of Pure and Applied Sciences, University of Tsukuba)

MRI was first proposed by Lauterbur in 1973[1] as an imaging method based on NMR principles. Since then, MRI has undergone remarkable technological development as well as clinical applications using mainly whole-body devices. Since the signal-to-noise ratio (S/N ratio) of MRI signals increases with the static magnetic field (or proton resonance frequency), the technological trend has been toward higher magnetic fields. Magnetic field strengths for whole-body MRI started at 0.04T [2] in the early 1980s, followed over the years by 0.35T, 1.5T [3], and 4T, and now up to 10.5T devices [4] are available for research use (although 1.5T and 3T devices are still the mainstream for clinical use).

Although MRI has thus continued to move toward higher magnetic fields, there has been a recent revival of MRI for human use at low fields (<0.5 T), ultra-low fields (10-100 mT), and very low fields (<10 mT) [5-7]. While this interest stems primarily from the urgent need to reduce the cost of MRI and improve access in medically underserved populations and developing countries, new point-of-care imaging applications, advances in hyperpolarization that allow imaging at low fields with high SNR, air-tissue interface and Imaging applications that reduce artifacts due to air-tissue interfaces and metallic implants are also reasons for this.

This talk will focus primarily on the hardware aspects of the paradigm shift from the former low field to high field and again from high field to low field, especially the unique opportunities and challenges that exist at low field strengths.

Reference

1) Lauterbur, PC. Image Formation by Local Induced Interactions: Examples Employing Nuclear Magnetic Resonance. Nature 1973;242,190-191.
2) Edelstein WA, Hutchison JMS, Johnson G, Redpath T. Spin Warp NMR Imaging and Applications to Human Whole-Body Imaging. Phys Med Biol 1980;25:751-756.
3) Hart HR, Bottomley PA, Edelstein WA, Karr SG, Leue WM, Mueller O, Redington RW, Schenck JF, Scott Smith L, Vatis D. Nuclear Magnetic Resonance Imaging: Contrast-to-Noise Ratio as a Function of Strength of Magnetic Field. AJR 1983;141: 1195-1201.
4) Nowogrodzki A. The world’s strongest MRI machines are pushing human imaging to new limits. Nature 2018;563,24-26.
5) Sarracanie M, Selameh N. Low-field MRI: how low can we go? A fresh view on an old debate. Frontier Physics 2020;8,1-14.
6) Wald LL, McDaniel PC, Witzel T, Stockmann JP, Cooley CZ. Low-cost and portable MRI. Journal of Magnetic Resonance Imaging 2020;52:686-696.

Measurement of Magnetic Resonance Signal without Prepolarization Technique at 1 mT

Daisuke Oyama
(Kanazawa Institute of Technology)

Introduction

Magnetic resonance imaging (MRI) in ultra-low magnetic field is one of expecting fields for new applications of MRI. We have been developed a compact ultra-low field MRI (ULF-MRI) systems composed of a desk size coil set. The measurement field in this system was several tens of micro-Tesla, therefore, a prepolarization pulse was used for increasing a signal intensity and controlling a direction of magnetic moments. However, using the prepolatization pulse results in increasing not only the signal intensity but also the recording time. In this study, we built and tested a new coil set for ULF-MRI system around 1 mT, aiming to realize the ULF-MRI system without the prepolarization technique.

Coil set for ULF-MRI

Fig. 1 shows a coil set for the 1 mT MRI system. The measurement field (B_0) coil was designed based on the Merritt coil[2] to generate uniform magnetic field. A radio-frequency (RF) coil was placed inside the B_0 coil. An induction coil to detect the magnetic resonance (MR) signal was placed at the center of the B_0 and RF coils, and these three coils were perpendicular to each other. This coil set was installed inside a magnetically shielded room.

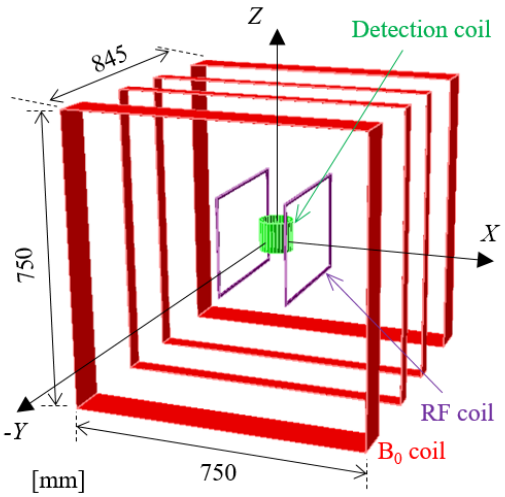

Fig. 1 Coil set for 1 mT MRI system.

Measurement of Magnetic Resonance Signal

Measurement of MR signal was demonstrated with a water sample. The density of B_0 was set to approximately 1 mT by applying electric current of 1.72 A to the coil. Fig. 2 shows the observed MR signal obtained by a spin-echo sequence. The echo time (TE) and the repetition period (TR) were 34 ms and 4.6 s, respectively.

Fig. 2 shows the measured signal with and without the water sample. These waveforms were obtained by applying a band-pass filter (40-46 kHz) and averaging 500 times. The echo signal clearly appeared in the waveform with water sample. The frequency of the echo signal was 42.5 kHz and it was in good agreement with the Larmor frequency of hydrogen at 1 mT. It was confirmed that the MR signal can be measured using the developed coil set at 1 mT.

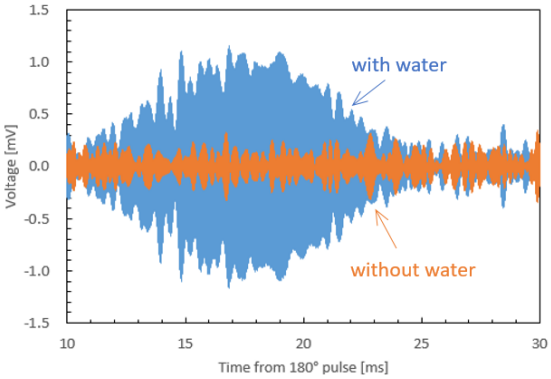

Fig. 2 Measured signals with and without a water sample.

Acknowledgements

This study was partly supported by KAKENHI (20K12680). This study partly includes some results of collaborative research with RICOH Co., Ltd.

Reference

1) D. Oyama et al., *IEEE Trans. Magn*., **53**, 5100504, 2017.
2) R. Merritt et al., *Rev. Sci. Instrum*, **54** (7), 879-882, 1983.

Ultra-low field MRI with an optically pumped magnetometer

T. Oida*, S. Hori**, T. Moriya*, A. Saito*, M. Suyama*, T. Kobayashi**
*Hamamatsu Photonics K.K., *Hirakuchi 5000, Hamakita-ku, Hamamatsu 434-8601, Japan*
**Kyoto University, *Kyoto-daigaku Katsura, Nishikyo-ku, Kyoto 615-8510, Japan*

In recent years, high-sensitivity magnetic field measurement using optically pumped magnetometers (OPMs) has attracted significant attention. Magnetic sensing with an OPM is performed by detecting electron spin precession in alkali metal vapors contained in a glass cell[1]. In general, OPMs are utilized in spin-exchange relaxation-free (SERF) conditions to detect low-frequency magnetic signals. In contrast, a high-density OPM cells require a large bias magnetic field along the pumping laser beam to tune the resonance frequency of the OPM to several tens or hundreds of kilohertz. Studies have reported that high-density OPMs are extremely sensitive outside the SERF condition[2, 3]. This high magnetic sensitivity of OPMs is suitable for MR signal detection in ultra-low-field magnetic resonance imaging (ULF-MRI). Consequently, an MR signal detector with an OPM and a flux transformer (FT) that serves to separate the magnetic condition between an MRI system and an OPM was reported by Savukov et al.[3]. In this study, we demonstrate ULF-MRI with a detector using an OPM and an FT.

To confirm if an MR signal detector with an OPM and an FT is feasible for ULF-MRI, we constructed an MR system with static field (B_0) of 7.05 mT, where the Larmor frequency of H_1 was 300 kHz. Subsequently, a cylindrical bottle phantom that contained 1 mmol/L gadopentetate dimeglumine (Bayer AG., MAGNEVIST) solution, was placed in the MR system to evaluate MR imaging with an OPM and an FT. A glass cell, circular polarized pump beam (DBR laser, PH770DBR040BF, Photodigm, Inc), and linear polarized probe beam (CatEye laser, CEL002, MOG Laboratories Pty Ltd) comprised the OPM sensor system. A 10 × 10 × 40 mm^3 glass cell containing potassium with He as the buffer gas and N_2 as the quenching gas was used as the sensor head. The He and N_2 gases in the cell were in the ratio He:N_2 = 9:1 at a pressure of 0.9 atm. The experiments were conducted after heating the cell to 180 °C to vaporize the potassium atoms. The electromagnetic shield for the OPM was a single-layer aluminum shield with two EMS panels (EMSPLM05, Medical Aid). In addition, the input coil was a 50-turn solenoid coil with a diameter of 5.6 cm, and the output coil was a Helmholtz type coil with a diameter of 2.6 cm and 10 turns on either side. The impedance of each coil was adjusted to 50 Ω at a frequency of 300 kHz. MR imaging was performed without pre-polarization, using a spin-echo sequence with TR = 300 ms, TE = 30 ms, FoV = 96 × 96 × 96 mm^3, matrix = 32 × 32 × 32, and NEX = 16 for a total scan time of 1 h 22 min. Additionally, the frequency response model of the OPM described by Kamada et al.[4] was used to correct the frequency responses of the OPM. Accordingly, sinusoidal fields of 290.00, 290.25, …, 310.00 kHz were measured by the detector with an an OPM and an FT.

However, the MR signals experienced distortions in the frequency domain owing to the narrow bandwidth of the OPM. Nevertheless, these distortions could be corrected using Kamada's frequency response model of the OPM. Furthermore, as a result of the 3D MR scan with a spatial resolution of 3 × 3 × 3 mm^3, MR images with a signal-to-noise ratio (SNR) of approximately 18 were obtained. However, large noises with specific frequencies were scattered across the diagonal area of the image.

In this study, we demonstrated the feasibility of an MR signal detector with an OPM and an FT. During measurement, the OPM exhibited a sensitivity of 14.7 fT/$Hz^{1/2}$ at 300 kHz, which is the center frequency of the MR signals. However, the frequency response of the OPM distorts the frequency-encoded MR signals. An appropriate frequency response correction was applied to obtain flat frequency responses. In future, rapid imaging and higher SNR of MR signal detection are expected to be achieved by optimizing the OPM and FT and/or suppressing the noise caused by the MR system.

Reference

1) D. Budker, and M. Romalis: *Nature Physics*, **3**(4), 227 (2007).
2) I.M. Savukov, S.J. Selzer, M.V. Romalis, K.L. Sauer: *Physical Review Letters*, **95**, 063004 (2005).
3) I.M. Savukov, V.S. Zotev, P.L. Volegov, M.A. Espy, A.N. Matlashov, J.J. Gomez, and R.H. Kraus Jr.: *J. Magn. Reason.*, **199**(2), 188 (2009).
4) K. Kamada, S. Taue, and T. Kobayashi: *Jpn. J. of Appl. Phys.*, **50**, 056602 (2011).

Nano-NMR technique based on NV center in diamond

S. Onoda[1] and J. Isoya[2]
[1]National Institutes for Quantum Science and Technology, Takasaki 370-1292, Japan
[2]University of Tsukuba, Tsukuba 305-8573, Japan

Nuclear magnetic resonance (NMR) spectroscopy is a promising technique for chemical analysis and molecular structure identification. Since it depends on the weak magnetic fields produced by a small thermal nuclear spin polarization, NMR suffers from poor molecule-number sensitivity. To overcome the low sensitivity, in 2013, a novel NMR technique based on Nitrogen-Vacancy (NV) centers in diamond has been proposed[1-2]. The statistical nuclear spin polarization rather than thermal polarization has utilized for nano-NMR of (nm)^3 samples. Compared to conventional NMR the number of nuclear spins required to generate a detectable signal is reduced by 12 orders of magnitude.

NV center is one of the numerous point defects in diamond. The most important features of the negatively charged NV centers is spin-state dependent photoluminescence at room temperature. A laboratory-built confocal microscopy (CFM) system is widely used to detect the photoluminescence from NV centers. A series of 532-nm laser excitation and microwave (MW) pulses are used for initialization, coherent manipulations, and readout of the electron spin-state of NV center. Fig. 1 (a) shows block diagram of CFM system for nano-NMR. Excitation laser (532 nm) and MW are pulsed by acousto-optic modulator (AOM) and MW switch. These are controlled by sequence/pulse generator. Pulsed laser is irradiated to diamond via an oil immersion objective lens (NA=1.3~1.4), and photoluminescence is detected by a single photon detector and fast counter after passing through a pinhole. Fig. 1 (b) shows the schematic draw of nano-NMR by NV center. The nuclear spins (^{1}H) in immersion oil are detected.

A dynamical decoupling technique based on the XY8-k pulse sequence which acts as a high-pass filter, to filter out low frequency noise is widely utilized for nano-NMR (Fig. 1(c)). This suppression of the noise source prolonged the electron spin coherence time of the NV centers by an order of magnitude or more. In addition to the noise suppression, the pulse sequence serves as a narrow-bandpass filter, revealing Larmor precession of the transverse magnetization of external nuclei. Signals from these statistically polarized nuclei are detected if their precession period matches the cycle of the π-pulse train applied to the NV centers. Fig. 1 (d) shows typical NMR signals of ^{1}H in immersion oil at the various k from 8 to 24. The higher number of k, the sharper signals because of narrow-bandpass filter. In 2013, the resolution was a few hundred thousand ppm, however, it has improved down to less than 1 ppm in more recent years. In this talk, the current progress as well as the basis of nano-NMR based on NV center in diamond are presented.

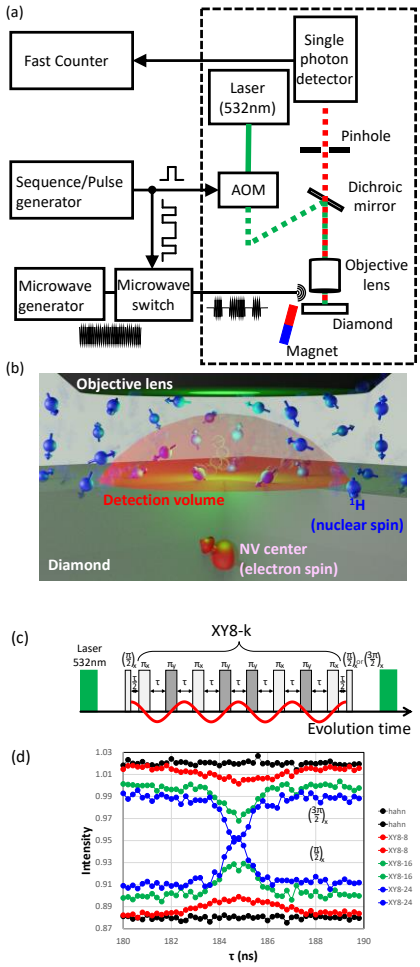

Fig. 1. (a) Block diagram of CFM system for nano-NMR, (b) schematic draw of ^{1}H nano-NMR, (c) XY8-k pulse sequence, and (d) typical ^{1}H-NMR signals at various k-values.

The authors would like to thank the financial supports by JST-DFG “Strategic Japanese-German Joint Research Project (SICORP)” from 2010 to 2013, and JSPS KAKENHI Grant Numbers 26220903, 26246001 and 21H04646. Part of studies on creation of NV centers was supported by MEXT Quantum Leap Flagship Program (MEXT Q-LEAP) Grant Number JPMXS0118067395 and JST Moonshot R&D Grant Number JPMJMS2062. We thank Prof. Dr. F. Jelezko and his group members for their help in measuring nano-NMR at university of Ulm, Germany.

References

1) T. Staudacher *et al.*, Science **339** (2013) 561., 2) H. J. Mamin *et al.*, Science **339** (2013) 557.

Development of compact proton magnetometer using TMR sensor

Kosuke Fujiwara, Hiroshi Wagatsuma and Seiji Kumagai
Spin Sensing Factory Corp.

The proton magnetometer operates as a magnetic sensor because the resonance frequency of NMR depends on the external magnetic field. Pulsed cutting of the magnetic field applied to a sample containing hydrogen ions causes magnetic relaxation of the protons, resulting in a free-induced decay (FID) signal. The magnitude of the magnetic field can be read by measuring the frequency of this FID signal. Since the proton magnetometer is based on the principle of frequency measurement, it is not easily affected by temperature, humidity, or individual differences in equipment, and can obtain measurement accuracy on the order of ppm. Due to their high measurement accuracy, proton magnetometers are used in fields such as subsurface and seafloor surveys and astrophysics.

A conventional proton magnetometer consists of a container of water or kerosene and a coil to apply a pulsed magnetic field and detect FID. It is difficult to miniaturize the conventional proton magnetometer because the FID signal decreases as the coil becomes smaller. In this study, we investigated the feasibility of a compact proton magnetometer by using tunnel magneto-resistance (TMR) sensor as the detection sensor of the FID signal. The TMR sensor is a highly sensitive magnetic sensor using magnetic tunnel junctions (MTJs), and its signal does not become smaller with miniaturization. In addition, the amount of water or kerosene as a signal source must be reduced in order to achieve a compact proton magnetometer. In this study, we verified the feasibility of a proton magnetometer when the volume of water is reduced to 1 cc.

The TMR sensor was deposited by a sputtering system and micro-fabricated by photo-lithography and argon ion milling. To improve the signal output of the TMR sensor, magnetic flux concentrators (MFCs) made of soft magnetic material was added. The size of the TMR sensor containing MFCs was 10 x 6.2 mm^2. The output of the TMR sensor was input to an oscilloscope and frequency counter through an amplifier circuit and a filter circuit. The sensor was placed in a coil for generating a pulsed magnetic field, and water in a plastic container was placed in the same coil. A large Helmholtz coil was placed outside the coil for the pulsed magnetic field, and the applied magnetic field from this Helmholtz coil was used as the external magnetic field. The magnitude of the external magnetic field was about 50 μT, assuming a geomagnetic field. The frequency of the FID signal in this case is approximately 2.1 kHz.

Fig.1 shows the results of frequency measurements with the TMR sensor when the magnitude of the external magnetic field is varied. The change in frequency corresponded linearly to the change in the external magnetic field. Fig.2 shows the repeatability of frequency when the amount of water is varied. Repeatability on the order of ppm was obtained in the 500 cc to 1 cc range, demonstrating the feasibility of a compact proton magnetometer using TMR sensor.

Acknowledgement
This study was supported by Acquisition, Technology & Logistics Agency (ATLA).

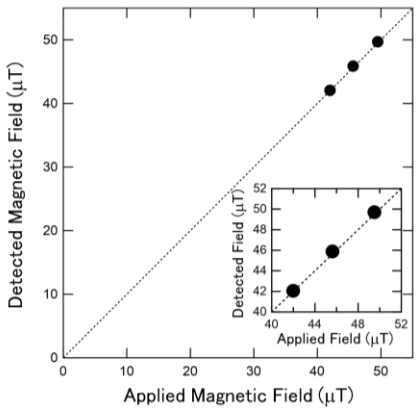

Fig.1 Change in frequency read by the TMR sensor when the external magnetic field is varied.

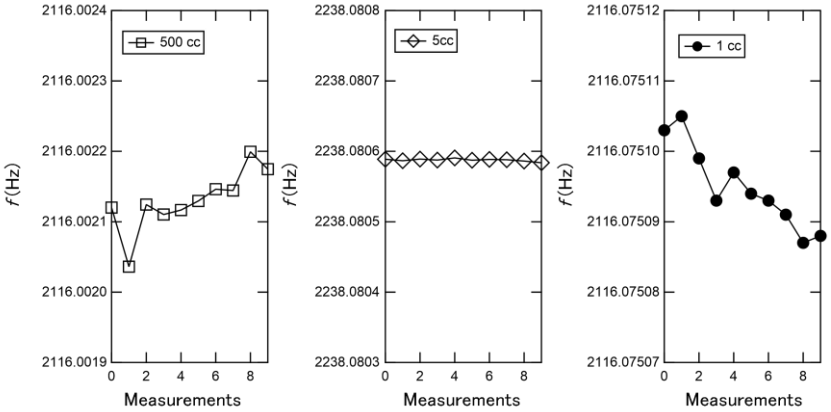

Fig.2 Repeatability of frequency measurements for 500 cc, 5 cc, and 1 cc volumes of water. Repeatability below 0.5 mHz was obtained for all water volumes.